Molecular Cell
Article

Small RNA Binding to 5′ mRNA Coding Region Inhibits Translational Initiation

Marie Bouvier,[1] Cynthia M. Sharma,[1,3] Franziska Mika,[1,3] Knud H. Nierhaus,[2] and Jörg Vogel[1,*]
[1]Max Planck Institute for Infection Biology, RNA Biology Group, Berlin D-10117, Germany
[2]Max Planck Institute for Molecular Genetics, AG Ribosomen, Berlin D-14195, Germany
[3]These authors contributed equally to this work
*Correspondence: vogel@mpiib-berlin.mpg.de
DOI 10.1016/j.molcel.2008.10.027

SUMMARY

Small noncoding RNAs (sRNAs) have predominantly been shown to repress bacterial mRNAs by masking the Shine-Dalgarno (SD) or AUG start codon sequence, thereby preventing 30S ribosome entry and, consequently, translation initiation. However, many recently identified sRNAs lack obvious SD and AUG complementarity, indicating that sRNA-mediated translational control could also take place at other mRNA sites. We report that *Salmonella* RybB sRNA represses *ompN* mRNA translation by pairing with the 5′ coding region. Results of systematic antisense interference with 30S binding to *ompN* and unrelated mRNAs suggest that sRNAs can act as translational repressors by sequestering sequences within the mRNA down to the fifth codon, even without SD and AUG start codon pairing. This "five codon window" for translational control in the 5′ coding region of mRNA not only has implications for sRNA target predictions but might also apply to *cis*-regulatory systems such as RNA thermosensors and riboswitches.

INTRODUCTION

Bacteria encode large numbers of small noncoding RNAs (sRNAs), most of which have been shown or predicted to act as antisense RNAs on *trans*-encoded target mRNAs (Majdalani et al., 2005; Romby et al., 2006; Storz et al., 2004). Translational repression has emerged as the primary mode of sRNA action and occurs at the level of translation initiation by sRNA binding to the 5′ untranslated region (UTR) of a target. Following the block of translation, some target mRNAs are irreversibly inactivated by endonucleolytic degradation (Darfeuille et al., 2007; Massé et al., 2003; Morita et al., 2006).

In bacteria, translation starts with the formation of an initiation complex consisting of 30S ribosomal subunits bound to the ribosomal binding site of the mRNA, fMET-tRNA^{fMet}, and initiation factors (Gualerzi et al., 2001; Laursen et al., 2005). Subsequently, 50S ribosomes bind, and the translationally active 70S ribosome complexes are formed. The purine-rich Shine-Dalgarno (SD) sequence, located several nucleotides upstream of the mRNA start codon (usually AUG) (Shine and Dalgarno, 1974), plays a key role in the initial capture of 30S ribosomes. It base pairs with a complementary anti-SD (aSD) sequence at the 3′ end of the 16S ribosomal RNA (Hui and de Boer, 1987; Jacob et al., 1987; Steitz and Jakes, 1975), enables the empty 30S subunit to associate on its own with mRNAs (Dontsova et al., 1991; Hüttenhofer and Noller, 1994; Ringquist et al., 1993), and helps position the start codon near the ribosomal peptidyl-tRNA (P) site (Calogero et al., 1988). A recent study of the structure of this so-called 30S/mRNA binary complex has underpinned the importance of the aSD-SD helix in the earliest phase of translational initiation (Kaminishi et al., 2007).

In order to repress translation initiation, an sRNA has to successfully compete with the 30S ribosome for target mRNA binding. It is therefore not surprising that most well-studied sRNAs base pair with the SD of their target(s) to render it inaccessible for pairing with the aSD sequence of the 30S. Masking of the target SD by the repressor sRNA was first proposed for *ompF* mRNA and MicF (Mizuno et al., 1984; Schmidt et al., 1995) and has since been amply supported by structural probing of diverse sRNA/mRNA complexes in vitro (e.g., Argaman and Altuvia, 2000; Geissmann and Touati, 2004; Huntzinger et al., 2005; Møller et al., 2002; Sharma et al., 2007; Udekwu et al., 2005). In addition, 30S toeprinting experiments assaying ternary complex formation in vitro provided strong evidence that several sRNAs inhibit their targets at the level of translation initiation (Argaman and Altuvia, 2000; Chen et al., 2004; Møller et al., 2002; Sharma et al., 2007; Udekwu et al., 2005).

An increasing number of bacterial sRNAs have recently been shown to repress multiple if not large sets of mRNAs (Guillier and Gottesman, 2006; Massé et al., 2005; Papenfort et al., 2006; Tjaden et al., 2006). In many of these cases, the kinetics of regulation strongly suggested that the mRNAs were directly targeted by an antisense mechanism. However, stable sRNA-target SD interactions could be predicted in only a few cases, posing the question of whether sRNAs can target other mRNA regions to successfully inhibit translation initiation. In fact, 30S subunits were early observed to cover an extended region on natural mRNA substrates (Murakawa and Nierlich, 1989; Platt and Yanofsky, 1975; Steitz, 1969), and subsequent detailed analyses of model mRNAs in complex with 30S and tRNA^{fMet} defined a ~40 nt ribosome coverage region (Beyer et al., 1994; Hüttenhofer and Noller, 1994) ranging from residue −20 in the 5′UTR to residue +19 in the coding sequence. Most of these contacts are by backbone and not sequence specific, whereas only the SD and start codon are sequence specific. More recently, X-ray and cryo-EM analysis of mRNA-ribosome complexes showed that translational-competent mRNA is

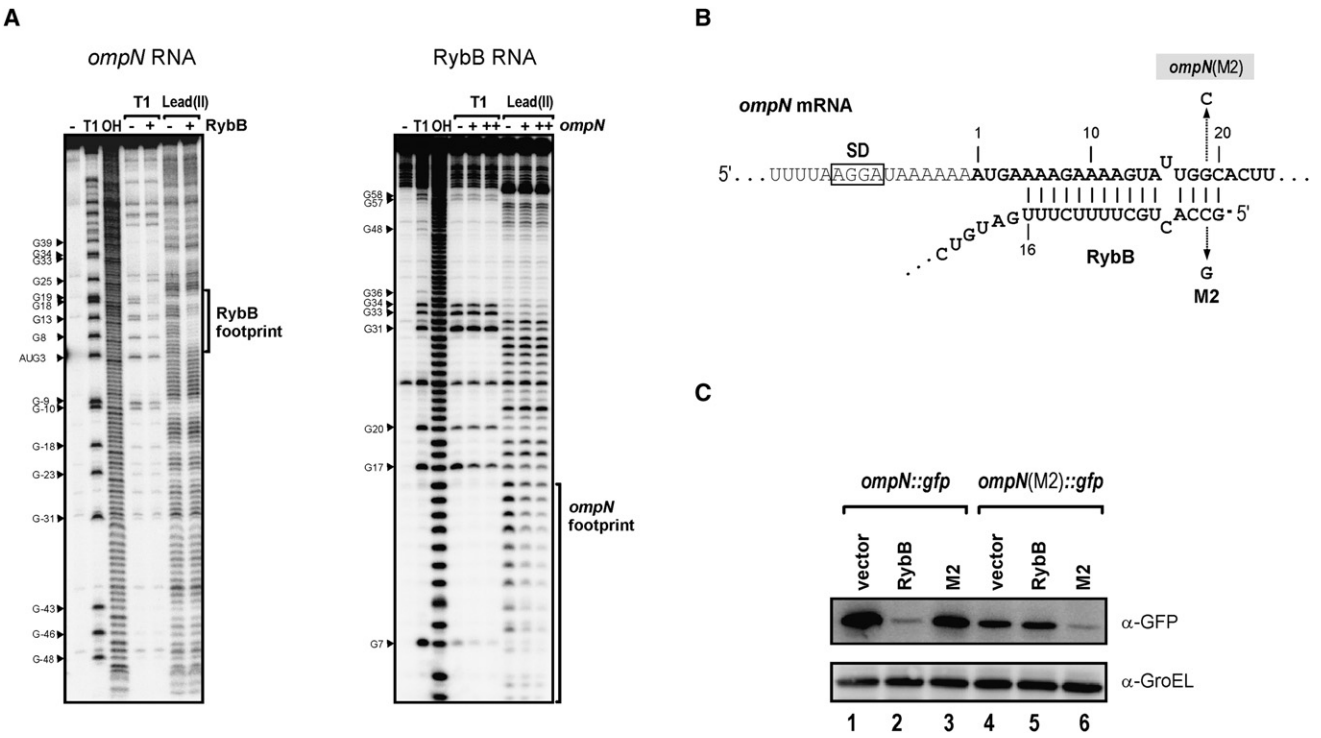

Figure 1. In Vitro and In Vivo Analysis of the RybB/*ompN* Interaction

(A) Structure mapping of RybB-*ompN* RNA complexes. The left autoradiogram shows structure probing with RNase T1 or lead(II), conducted on a 5′ end-labeled *ompN* mRNA fragment corresponding to the −75 to +90 region. Plus and minus symbols indicate the presence and absence, respectively, of unlabeled RybB RNA (50-fold excess). The right autoradiogram shows the reciprocal experiment, i.e., probing of 5′ end-labeled RybB RNA in the absence (−) or presence (+ or ++, 25- or 50-fold excess, respectively) of unlabeled *ompN* RNA. (T1) RNase T1 cleavage under denaturing conditions; (OH) alkaline ladder; (−) mock-treated control RNA. Some nucleotide positions are given for orientation left to the gels; numbering of *ompN* residues is relative to A of AUG start codon. The RybB- or *ompN*-induced footprints, i.e., regions with reduced cleavage upon addition of the unlabeled partner RNA, are indicated by vertical bars to the right.

(B) RybB/*ompN* interaction determined by the probing experiments above and supported by prediction with the *RNAhybrid* algorithm (Rehmsmeier et al., 2004). The *ompN* CDS and the RybB RNA sequence are set in boldface. Arrows indicate complementary base pair changes (point mutations yielding M2 variants of RybB or *ompN*) introduced in the sRNA expression and *ompN* fusion plasmids below.

(C) RybB-dependent regulation of a *Salmonella ompN::gfp* fusion in vivo. Western blot analysis of *E. coli* strain JVS-2398 harboring either wild-type *ompN::gfp* (pFM7-5) or mutant *ompN*(M2)*::gfp* (pFM33-1) fusion plasmids, in combination with sRNA control vector, pJV300, or plasmids expressing the RybB wild-type (pFM1-1) or M2 mutant (pFM17-2) RNAs. Changes in OmpN::GFP protein levels were detected using a α-GFP antibody (upper panel). GroEL served as loading control (lower panel).

unfolded in the 5′ coding sequence (CDS) (Marzi et al., 2007; Yusupova et al., 2001).

We show in this paper that the conserved RybB sRNA represses translation of one of its previously proposed targets, the *Salmonella ompN* mRNA (Papenfort et al., 2006), by forming a short duplex with the *ompN* CDS. This interaction, albeit it does not sequester the *ompN* SD or AUG sequences, suffices to inhibit ternary complex formation, presumably by steric hindrance. The results of systematic antisense scanning of the 5′ CDS of diverse mRNAs suggest a rule for codon region targeting such that interactions down to the fifth codon will likely repress the target mRNA at the level of translation initiation.

RESULTS

RybB Forms a 4 + 11 bp RNA Duplex with the *ompN* mRNA Coding Region

The ~80 nt RybB sRNA was recently identified as a factor that limits the synthesis of new outer membrane proteins (OMPs) in the envelope stress response of enterobacteria (Johansen et al., 2006; Papenfort et al., 2006; Thompson et al., 2007). *Salmonella* RybB was shown to repress more than 10 *omp* mRNAs at the posttranscriptional level, but the underlying molecular mechanism remained unclear. We showed that the 5′ region (−73 to +89) of one of these targets, *ompN* mRNA, formed a singular complex with RybB RNA (apparent K_D < 50 nM) under standard in vitro conditions, suggesting that the two RNAs interacted directly (Papenfort et al., 2006). To map the putative RNA interaction sites, the two RNAs, either alone or in combination, were subjected to structure probing by RNase T1 or lead (Pb^{2+})-induced cleavage (Figure 1A). Unlabeled RybB RNA protected a 16 nt region on 5′ end-labeled *ompN* RNA from cleavage. This "footprint" is most clearly seen with lead probing and spans from residue A_5 to C_{20} of the *ompN* CDS. Reciprocally, probing of labeled RybB in complex with unlabeled *ompN* RNA suggested that the 5′ part of RybB down to residue U_{16} engages in the interaction. Notably, there were no significant changes in other parts of *ompN* or RybB RNA. Alignment of the protected residues

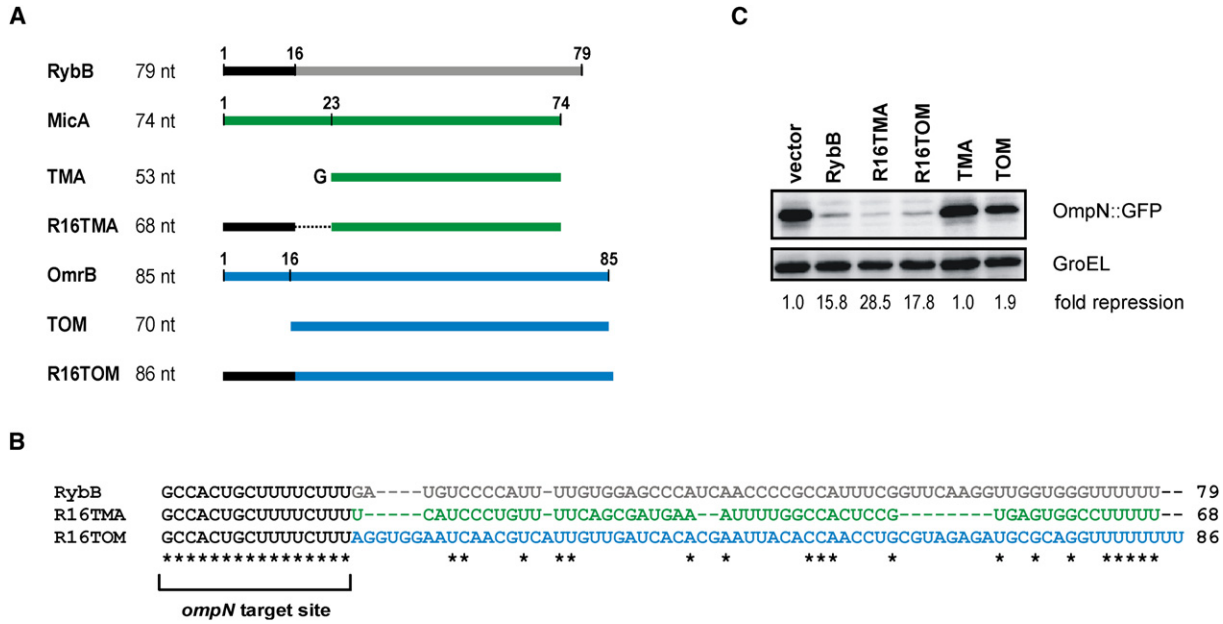

Figure 2. The First 16 Residues of RybB Are Sufficient for *ompN* Repression

(A) Schematic drawing of chimera RNAs (R16TMA, R16TOM) constructed by fusions of the 16 5′ end residues of RybB to truncated versions (TMA, TOM) of *Salmonella* MicA and OmrB sRNAs. Horizontal bars and a color code indicate RybB, MicA, and OmrB RNA fragments. Expected transcript sizes upon in vivo expression of the RNAs are given in nucleotides. Numbers above the bars denote sequence positions relevant for chimera construction. For stable expression of TMA RNA, a G residue was added to the 5′ end upon MicA truncation.

(B) Alignment of RybB, R16TMA, and R16TOM RNA sequences shows that sequence identity is limited to the transplanted 16 residues of RybB. Stars indicate common nucleotides.

(C) RybB and the above-described chimeric and truncated RNAs were assayed for their ability to regulate OmpN::GFP synthesis as in Figure 1C. Shown is a western blot analysis of GFP from *E. coli* cells carrying the *ompN::gfp* fusion plasmid in combination with control or sRNA expression plasmids as indicated above the lanes (from left to right: pJV300, pFM1-1, pFM46-1, pFM100-2, pFS135, pFS134). Fold repression of OmpN::GFP synthesis by the tested RNAs in comparison to sRNA control vector, pJV300, is indicated below the lanes and was calculated from OmpN::GFP band intensity and normalized to GroEL signals.

predicts that RybB forms a 4 + 11 bp RNA duplex with the *ompN* CDS (Figure 1B).

To validate the RybB-*ompN* interaction in vivo, we constructed a translational *ompN* fusion to the NH_2 terminus of green fluorescent protein (GFP). The 5′ region of *ompN* mRNA (−75 to +87 relative to AUG) was cloned into a low-copy *gfp* fusion vector, pXG10 (Urban and Vogel, 2007); the resulting *ompN::gfp* fusion is constitutively transcribed to specifically assay posttranscriptional regulation. We also constructed a compatible plasmid, pP_L-RybB, which expresses the native *Salmonella* RybB RNA from a constitutive $P_{LlacO-1}$ promoter (Lutz and Bujard, 1997). Next, *E. coli* Δ*rybB* cells carrying the *ompN::gfp* fusion were cotransformed with either pP_L-RybB or the sRNA control vector, pJV300 (Urban and Vogel, 2007), and RybB-dependent regulation was determined by quantification of OmpN::GFP fusion protein levels. Figure 1C shows that plasmid pP_L-RybB severely curtailed *ompN::gfp* expression (~14-fold repression; compare lanes 1 and 2), confirming that RybB regulates *ompN* mRNA in the 5′ region. Subsequently, point mutations were introduced in the two interacting RNAs (Figure 1B): change of C2 to G in RybB yielded the M2 mutation, and change of G + 19 to C the compensatory *ompN*(M2) allele. Fusion regulation was lost when the single mutants, RybB-M2 (which accumulated to the same level as wild-type RybB; see Figure S1 available online) or *ompN*(M2)*::gfp*, were combined with the wild-type allele of the other RNA (Figure 1C, lane 3 or 5) yet restored for *ompN*(M2)*::gfp* upon coexpression of the compensatory M2 RNA version of RybB (lane 6). These in vivo experiments confirmed that RybB represses the *ompN* mRNA by an antisense mechanism that requires the very 5′ region of RybB.

The Short RybB-*ompN* Interaction Is Sufficient for mRNA Repression In Vivo

The above structure probing suggested that only the first 16 residues of RybB pair with *ompN* mRNA. If so, transplantation of this short RybB region onto noncognate sRNAs should create *ompN* regulators, an approach previously used by Gerdes and colleagues to validate the limited base pairing of *sok* antisense RNA to *hok* toxin mRNA (Franch et al., 1999). To test this, we constructed plasmids expressing chimeras of the RybB 5′ end with truncated versions of the structurally unrelated *Salmonella* MicA and OmrB sRNAs (Figure 2A). MicA is a 74 nt sRNA that represses the *ompA* and *lamB* mRNAs (Bossi and Figueroa-Bossi, 2007; Rasmussen et al., 2005; Udekwu et al., 2005), and OmrB (86 nt) was previously shown in *E. coli* to regulate multiple targets, but not *ompN* mRNA (Guillier and Gottesman, 2006; Tjaden et al., 2006). In the chimeric R16TMA and R16TOM RNAs, the RybB 5′ end (residues 1–16) was fused to residues 23–74 of MicA or 1686 of OmrB, respectively. Alignment of the R16TMA, R16TOM, and RybB RNAs shows that they share little

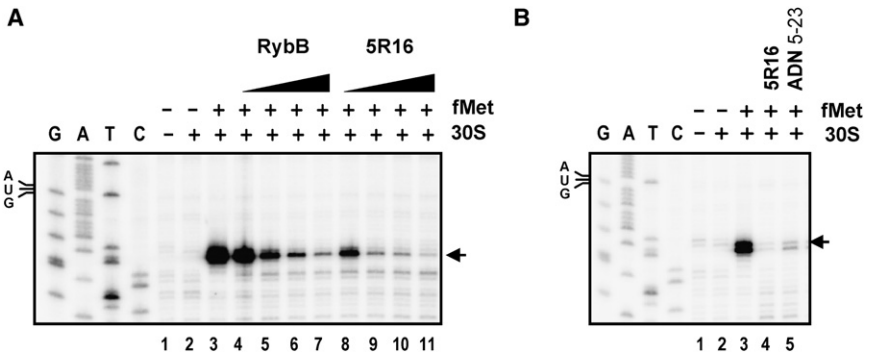

Figure 3. The RybB 5′ End Inhibits Translation Initiation on the *ompN* mRNA In Vitro

(A) 30S ribosome toeprinting and control reactions (lanes 1–11) were carried out on 0.2 pmol *ompN* RNA as described in the Experimental Procedures. "−/+" denotes absence/presence of 2 pmol 30S subunits and/or initiator $tRNA^{fMet}$ in the reactions. The GATC lanes correspond to sequencing ladders generated with the same reverse transcription primer as used in the toeprint reactions. The position of the *ompN* AUG start codon is marked to the left. The arrowhead on the right indicates the 30S toeprint. Increasing concentrations of RybB RNA (0.2, 0.6, 1, or 2 pmol) gradually weaken the 30S toeprint signal (lanes 4–7). The 30S toeprint is also inhibited by addition of 5R16, a short RNA oligo identical to the first 16 nt of RybB (lanes 8–11, 0.2, 0.6, 1, or 2 pmol).

(B) Comparison of toeprint inhibition by 5R16 RNA or a DNA 19-mer (ADN 5-23) antisense to residues 5–23 of the *ompN* CDS. Both oligos (2 pmol; lanes 4 and 5) inhibit 30S binding to *ompN* RNA (0.2 pmol).

if any sequence similarity outside the common RybB residues 1–16 (Figure 2B). The chimeric R16TMA and R16TOM RNAs, when expressed from a P_L promoter in vivo, repressed the *ompN::gfp* fusion as effectively as wild-type RybB (Figure 2C, lanes 2–4). In contrast, expression of the MicA- or OmrB-derived backbones alone, i.e., TMA or TOM (Figure 2A), had negligible effects on the *ompN::gfp* fusion (Figure 2C, lanes 5 and 6). Northern blot analyses have shown that all chimeric and control sRNAs accumulate to the same level as wild-type RybB (F.M., C.M.S., M.B., and J.V., unpublished data). Thus, we concluded that the pairing of the RybB 5′ end to the CDS of *ompN* mRNA is fully sufficient for target regulation in vivo.

RybB Binding to the *ompN* CDS Inhibits Translational Initiation In Vitro

The experiments so far suggested that *ompN* mRNA is targeted exclusively in the CDS, but without masking the two major mRNA elements for 30S ribosome association, SD and AUG (Figure 1B). Whether RybB could still inhibit translation initiation was tested in 30S ribosome toeprinting assays (Hartz et al., 1988). The *ompN* mRNA fragment was annealed to an end-labeled primer complementary to the *ompN* CDS, and incubated with 30S subunits in the presence or absence of uncharged $tRNA^{fMet}$, followed by cDNA synthesis. Analysis of the extension products (Figure 3A) revealed one ribosome-induced, $tRNA^{fMet}$-dependent termination site at the characteristic +16 position (lane 3). This "toeprint" signal was decreased in a dose-dependent manner when increasing concentrations of RybB RNA were added prior to incubation with 30S/fMet (lanes 4–7), suggesting inhibition of initiation complex formation. In contrast, the noncognate MicA sRNA failed to decrease the *ompN* toeprint signal (data not shown), indicating that 30S binding to *ompN* was specifically inhibited by RybB.

To test if the 4 + 11 bp RNA duplex of RybB with the *ompN* CDS by itself sufficed for translational inhibition, a short RNA consisting of only the first 16 nt of RybB was chemically synthesized and tested as above (lanes 8–11). This RNA, 5R16, also inhibited ternary complex formation in a dose-dependent manner. In fact, at all four concentrations tested, 5R16 decreased the toeprint signal 4-fold more than did full-length RybB RNA. We do not currently know whether faster/tighter binding makes 5R16 RNA a stronger inhibitor. Nonetheless, the result obtained with 5R16 showed that RybB antisense pairing limited to the *ompN* CDS can block translation initiation; in other words, 30S entry is inhibited although SD, and AUG start codons are free to base pair.

Antisense Scanning Approach Reveals an Extended *ompN* CDS Region for 30S Inhibition

DNA oligonucleotides antisense to 5′UTRs were previously observed to effectively inhibit the translation of *E. coli ompA* or *ompC* mRNA in 30S toeprinting assays (Chen et al., 2004; Vytvytska et al., 2000). Thus, we tested whether a DNA oligo complementary to the *ompN* CDS (+5 to +23) could substitute for an antisense RNA as inhibitor. This DNA oligo inhibited the *ompN* toeprint almost as strongly as 5R16 RNA when provided in 10-fold excess over *ompN* mRNA (Figure 3B).

We then used such short DNA oligos to fine map the boundary for effective translational repression at the *ompN* CDS. Similar to the antisense oligonucleotide-scanning approach by Johansson et al. (1994), who systematically blocked eukaryotic mRNAs to study inhibition of translation, we sequestered the *ompN* CDS with a series of DNA oligos starting from position +5, and in one base pair steps down to position +20 (Figure 4A). Oligos were preannealed to *ompN* mRNA, and ternary complex formation was determined in toeprinting assays as above (Figure 4B). Toeprint intensity curves from three independent experiments show that 30S binding was strongly inhibited by antisense oligos which paired to the regions starting from +5 through +12 of *ompN* mRNA (lanes 4–12). The oligo starting at position +13 still gave 50% inhibition (lane 13), whereas inhibition was consistently lost at all tested downstream positions (lanes 14–19). Thus, an extended region of the *ompN* CDS is sensitive to antisense-mediated translational control.

CDS Targeting Represses mRNAs Unrelated to *ompN* and Is Independent of SD Structure

According to our structure-probing data (Figure 1A), the CDS of *ompN* mRNA is unstructured. If specialized structure is no requirement for CDS targeting, then any other mRNA might as well be repressed by antisense coverage of the 5′ coding region. To address this, the *gltI* and *ompC* mRNAs known to be amenable to toeprinting (Chen et al., 2004; Sharma et al., 2007)

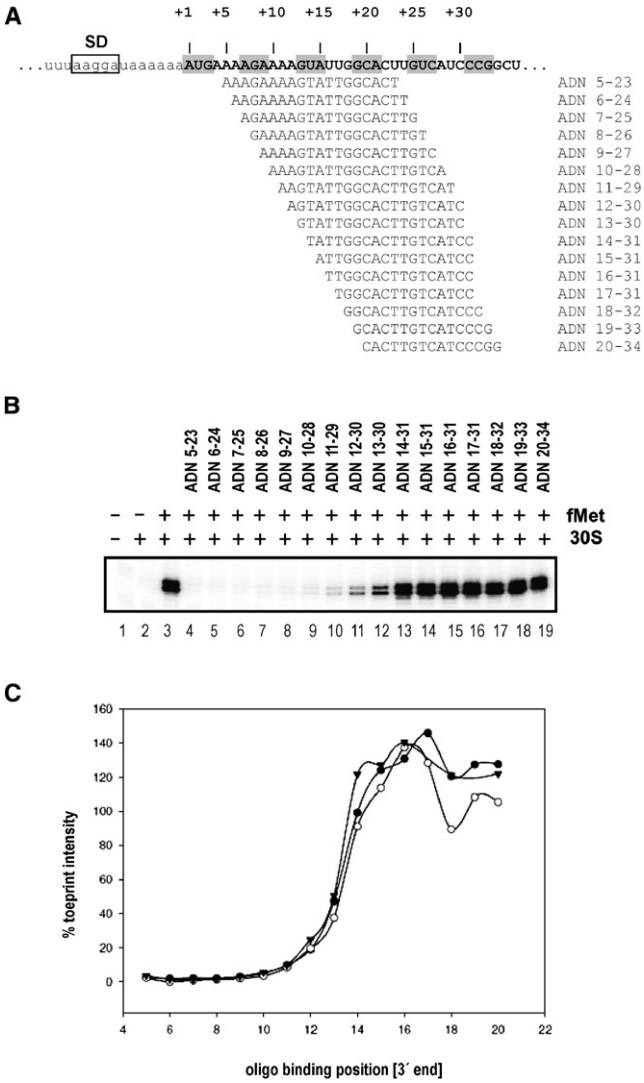

Figure 4. Antisense Scanning Reveals an Extended Region of the *ompN* CDS Sensitive to Translational Repression

(A) Overview of the positions of DNA antisense oligos used to mask the *ompN* 5′ CDS in the toeprinting assay below. Oligo sequences are given as the complement to facilitate better comparison with the *ompN* mRNA sequence shown at the top. Oligo names are given to the right. Shading indicates odd numbered *ompN* codons.

(B) Shown are 30S ribosome toeprint formation (lane 3), 30S ribosome toeprint inhibition by DNA antisense oligos (lanes 4–19), and control reactions (lanes 1 and 2). Concentrations of *ompN* mRNA fragment, 30S subunit, and $tRNA^{fMet}$ were as in Figure 3B. In lanes 4–19, the antisense oligos shown in (A) were added in 10-fold excess over *ompN* mRNA. The section of the autoradiogram of the gel that contains the 30S toeprint signal is shown.

(C) Intensities of toeprint signals of three independent experiments were quantified and plotted over the starting positions of antisense oligo complementary with the *ompN* CDS. For each experiment, the signal obtained in the absence of antisense oligos (e.g., lane 3 in [B]) was set to 100%.

were subjected to the antisense scanning approach described above (Figures 5A and 5B). We found that antisense oligos extending into the first four codons of *gltI* mRNA strongly inhibited the toeprint signal, and that 50% inhibition was still achieved around position +11. In the case of *ompC* mRNA, the window for repression was narrower, i.e., only oligos down to position +9 (third codon) gave more than >50% inhibition.

All three tested mRNAs share an AUG start codon (Figure 5C), which makes it unlikely that the observed variability of the window for antisense inhibition relates to initiator tRNA pairing. Alternatively, can the relative position or composition of the SD affect which part of the coding region is sensitive to antisense inhibition? Based on complementarity to residues 1540–1537 of 16S rRNA (numbering acc. to *E. coli*), we assume that the AGGA and AGGG tetramers located at positions −11 of the *ompN* or −12 of the *ompC* start codon constitute the respective SD sequences; thus the relative SD positions differ by 1 nt. In contrast, the position at which CDS targeting supports >50% inhibition of 30S binding differs by 4 nt (*ompN*, +13; *ompC*, +9; Figure 5B). To test whether the SD contributes to the positional variability of CDS targeting, the SD sequences of the two mRNAs were swapped, yielding the *ompN* SD-C and *ompC* SD-N mutant mRNAs (Figure 5C). In toeprinting assays, the SD mutant mRNAs yielded 30S inhibition curves almost congruent with that of their respective wild-type mRNA (Figure 5B and Figure S2). Thus, neither the composition nor the exact SD position affects which region of the CDS is sensitive to antisense inhibition. In addition, the *gltI* SD is located at the same upstream position as in *ompN* (Figure 5C), yet CDS sensitivity to antisense block differs by at least two nucleotides (Figure 5B). Differential pairing properties of the antisense oligos used for the various mRNAs are unlikely to cause the shift in CDS sensitivity, since all oligo sets have similar melting temperatures (Table S1). Therefore, overall mRNA sequence rather than SD or AUG pairing is likely to determine which part of the CDS needs to be targeted to prevent 30S binding.

Evidence for a Five Codon Window of Translational mRNA Repression by sRNA

The results obtained so far suggested a five codon window within which sRNAs must bind in order to operate as translational repressors in the 5′ CDS. They also predicted that *ompN* mRNA translation should no longer be repressed by RybB sRNA if the target site were moved downstream of the fifth codon. To validate this hypothesis, we gradually shifted the RybB target site by inserting the corresponding residues of the *gltI* CDS immediately downstream of the *ompN* AUG start codon, a strategy meant to minimize potential structural perturbations around both the *ompN* SD and the RybB-binding sequence (Figure 6A). Inserted sequences were evaluated for potential alternative base pairing with RybB and, if necessary, mutated further.

The *ompN* mutant mRNAs were toeprinted in the absence or presence of RybB, and RybB-mediated inhibition was compared to *ompN* wild-type mRNA (Figure 6B). Interestingly, insertion of the diverse *gltI* residues tends to decrease the basal toeprint signal of the chimeric mRNAs, indicating that the purine-rich first *ompN* codons favor 30S binding. Nevertheless, calculation of inhibition factors showed that RybB failed to inhibit 30S binding when the interaction site was shifted downstream of the fifth codon (Figure 6C). In contrast, the chimeric *ompN*[B + 17] mRNA could be specifically repressed both in vitro by antisense masking of the synthetic CDS sequence and in vivo by a synthetic

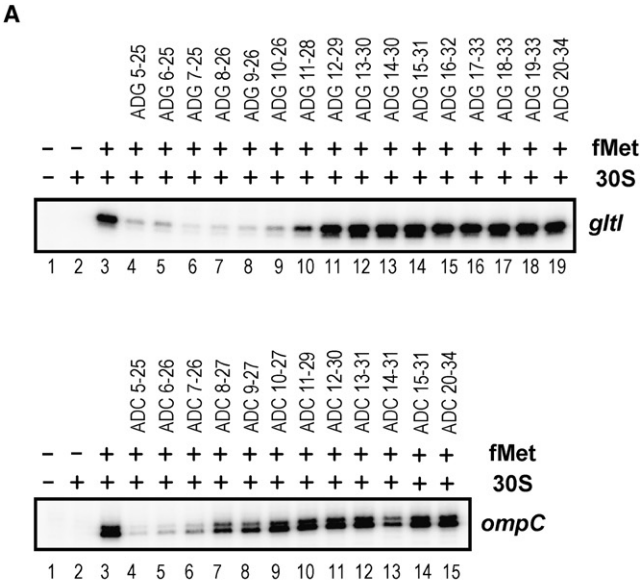

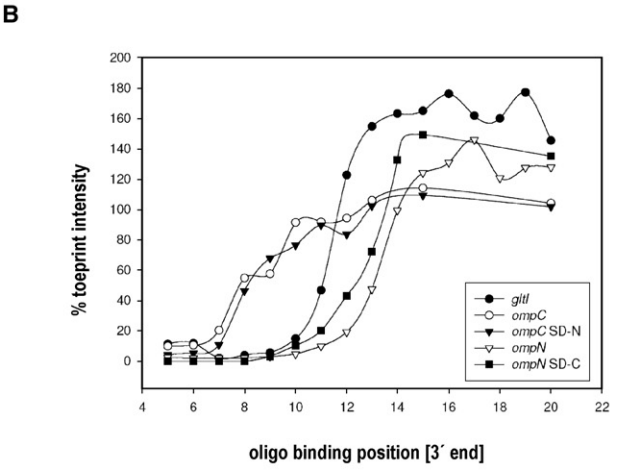

C

gltI	UGAUAA**AGGAG**UUGGAU**AUG**
ompC	AACAG**AGGG**UUAAUAAC**AUG**
ompC SD-N	AACAUA**AGGA**UAAUAAC**AUG**
ompN SD-C	UUUUG**AGGG**UUAAAAAA**AUG**
ompN	UUUUUA**AGGA**UAAAAAA**AUG**

Figure 5. Antisense Scanning of *gltI* and *ompC* mRNAs Supports a Five Codon Window Translational Control at the CDS

(A) 30S ribosome toeprinting (lanes 3–19) and control reactions (lanes 1 and 2) as in Figure 4B but on 5′ fragments of *gltI* mRNA (0.2 pmol) or *ompC* mRNA (0.2 pmol). Note that, unlike in the experiment with *ompN* and *gltI* mRNAs, antisense scanning was limited to a set of 12 oligos for *ompC*. Reactions contained 2 pmol of 30S subunit and/or $tRNA^{fMet}$ (where indicated). Antisense oligos ("ADG" for *gltI* or "ADC" for *ompC*) were added in lanes 4–19 or 4–15, respectively. The extension of the oligo name denotes the region of antisense complementarity with the *mRNA* CDS; e.g., ADG5-21 is fully complementary to the +5 to +21 region of *gltI* mRNA. The section of the autoradiogram of the gel that contains the 30S toeprint signals is shown.

(B) Toeprint signal intensities of antisense scanning experiments of *gltI*, *ompC*, and the chimeric *ompC* SD-N and *ompN* SD-C mRNAs were quantified and plotted as in Figure 4C. Raw data obtained for the antisense scanning of *ompC* SD-N or of *ompN* SD-C mRNAs are provided in the Supplemental Data (Figure S3). The *ompC* toeprint signal obtained in lane 13 (oligo ADC 14–31) was not plotted; the aberrant inhibition by this oligo is likely due additional binding to the *ompC* 5′UTR.

(C) Alignment of −17 to +3 regions of the various mRNAs used for the antisense scanning experiments. Putative SD sequences are underlined.

sRNA designed to be complementary to AUG proximal sequence (Figure S3), suggesting that the chimeric mRNAs reflect properties of the *ompN* wild-type mRNA.

To rule out that failure to inhibit the mutants with downstream RybB sites resulted from impaired RybB binding, complex formation of RybB with the *ompN* wild-type or selected mutant mRNAs (B + 11, B + 15, B + 16, B + 17, and B + 20) was assayed in gel retardation experiments. The position of the RybB site had little if any effect on target binding (Figure S4). Therefore, loss of 30S repression at these downstream sites is best explained by RybB binding outside the five codon window in which a sRNA can effectively repress translation initiation.

DISCUSSION

The present study has identified an example of an sRNA that represses a *trans*-encoded mRNA by sequestering the 5′ proximal part of the CDS of the target downstream of the AUG. Structure probing of RybB/*ompN* RNA complexes in vitro (Figure 1) revealed an ~16 bp RNA duplex formed by RybB with the *ompN* CDS. Compensatory base pair changes introduced in RybB and an *ompN* fusion mRNA validated this interaction in vivo. Transplantation of the 16 interacting RybB nucleotides to noncognate sRNAs created specific *ompN* regulators of the same potency as wild-type RybB RNA. Collectively, these data provide strong evidence that *ompN* is targeted exclusively at the CDS, i.e., without antisense pairing to the *ompN* SD or AUG. Despite the lack of sequence-specific SD and AUG contacts, repression occurs at the level of translation initiation, i.e., both full-length RybB RNA and a 16 nt RybB-derived RNA antisense to only the *ompN* CDS invariably inhibit 30S association of the *ompN* mRNA in vitro.

In the canonical pathway of translational inhibition, regulatory sRNAs compete with the 30S subunit for binding to the nascent target mRNA. One may argue that owing to their typically weak, imperfect target interactions, *trans*-encoded sRNAs may stand a better chance to inhibit translation by preventing initial 30S entry at the 5′ end of an mRNA than by competing with the strong RNA helicase activity of elongating 70S ribosomes (Takyar et al., 2005) at a downstream mRNA position. Two adjacent mRNA sequences, i.e., SD and AUG, are key elements for the formation of the early translation initiation complex, and many previous studies focused on sRNA regulators with complementarity to this narrow mRNA region. However, there is accumulating evidence that sRNAs may also select other regions of mRNAs to prevent translation initiation. First, whereas the number of identified sRNAs has grown at a staggering rate, and ever more sRNAs are proposed to target large sets of cellular mRNAs (Lease et al., 2004; Massé et al., 2005; Papenfort et al., 2006; Tjaden et al., 2006), relatively few of these RNAs possess obvious

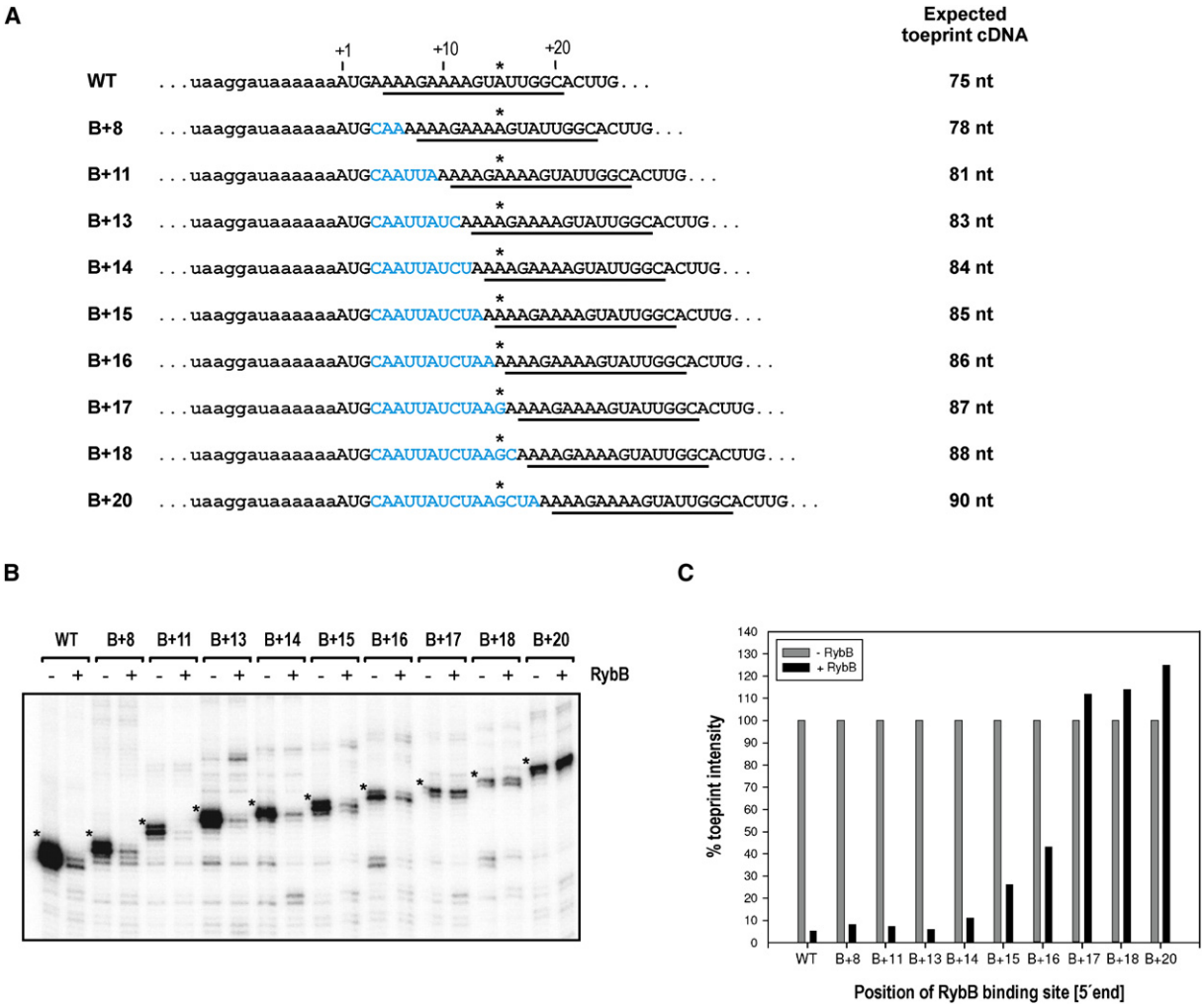

Figure 6. Shift of the RybB-Binding Site Corroborates the Five Codon Window for Translational Control

(A) Overview of the position of the shifted RybB binding site (underlined) in chimeric *ompN* RNAs. Blue letters denote nucleotides inserted downstream of *ompN* position +3. Expected cDNA length for reverse transcriptase stop at the bound 30S (indicated by a star above the mRNA sequence) in the toeprinting assay is specified to the right. Note that the position of RybB site in native *ompN* is B + 5.

(B) 30S toeprint formation in the absence (−) or presence (+) of RybB. Concentrations of *ompN* mRNA, 30S subunit, and $tRNA^{fMet}$ were as in Figure 3B. RybB was added in 10-fold excess over *ompN* mRNA. The section of the autoradiogram of the gel that contains the 30S toeprint signals is shown.

(C) Intensities of toeprint signals were quantified. For each *ompN* leader, the signals obtained in the absence of RybB were set to 100%. Percents of toeprint inhibition were determined as the ratio between the toeprint intensities in the presence of RybB and the toeprint intensities in the absence of RybB. Data obtained are summarized in this histogram.

antisense-SD or anti-AUG sequences. Second, biochemical and structural studies of 30S ribosome-mRNA complexes showed that a significant part of the 5′ CDS of mRNAs has to be accommodated into the mRNA tunnel of 30S subunits and thus needs to be, or be rendered to be, single stranded for efficient translation initiation (Marzi et al., 2007; Yusupova et al., 2001). Fine mapping of the mRNA space covered by the 30S subunit revealed the first 19 residues (or six codons) of these mRNAs to be in close contact with 30S (Beyer et al., 1994; Hüttenhofer and Noller, 1994). The crystal structure of a ribosome-bound mRNA showed that downstream residues (positions approximately +7 to +10) pass through a layer of ribosomal RNA, and it was suggested that this helps to position the mRNA immediately downstream from the start codon. Third, detailed analysis of the autoregulation of the synthesis of the *E. coli* ribosomal protein L35 and L20 (encoded by *rpmI-rplT*) indicated that translational repression involves the formation of double-stranded RNA structure physically located downstream of the *rpmI* AUG (Chiaruttini et al., 1996).

The RybB-*ompN* interaction falls well within both the previously mapped window of 30S contacts with mRNAs in vitro (−20 to +19 region) (Beyer et al., 1994; Hüttenhofer and Noller, 1994) and the positional constraints that can be predicted from the now-available crystal structures of ribosome-mRNA complexes (Yusupova et al., 2001). Whereas sterical hindrance of ribosomes by RNA structure was documented in the 5′UTR,

e.g., in *copT* mRNA (Malmgren et al., 1996), it had been unclear which region downstream of the start codon would be sensitive to translational repression by stable RNA pairing. We sought to define this border by systematic coverage of diverse mRNAs in their 5′ coding regions. The results obtained on three unrelated mRNAs reproducibly showed that antisense inhibition of 30S binding can only take place within the first five codons. The position of 50% toeprint inhibition varied among the tested mRNAs, from approximately + 9 (*ompC*) to +13 (*ompN*). We tend to explain these variations by looser or tighter contacts of the individual mRNAs at the edge of their downstream 30S interaction, since all tested mRNAs were correctly positioned by $tRNA^{fMet}$/AUG pairing in the ternary translational initiation complex (evidenced by the consistently observed toeprint at +15/+16). Regardless of these variations, the most downstream position observed in our 30S inhibition experiment involving antisense oligos, i.e., +13 (*ompN*), suggests a window for antisense control narrower than expected from previous 30S footprinting data (Hüttenhofer and Noller, 1994). However, the window for the natural sRNAs that typically range in length from 50 to 200 nt may be slightly extended by protruding nucleotides located downstream of the core interaction. The shift of the 50% inhibition point from +13 obtained with antisense masking of the natural *ompN* mRNA (Figure 4C) to +16 when natural RybB RNA was used to target diverse *ompN* mutant mRNAs (Figure 6C) is in favor of such a scenario. However, given that the many unpaired RybB residues (nucleotides 17–80; ~80% of RybB) are spatially well positioned toward start codon and SD of *ompN* mRNA, their contribution to translational repression still seems to be modest.

First results obtained with reporter fusion of chimeric *ompN* mRNAs support that RybB-mediated repression is specific to the AUG-proximal CDS but also suggest that there may also be slight variations to the theme in an in vivo situation. That is, when we tested *gfp* reporters of the chimeric B + 8, B + 11, B + 14, B + 17, and B + 20 *ompN* mRNAs, we observed that RybB-mediated repression in vivo was totally lost at +20 (Figure S5) as compared to +17 in vitro (Figure 6C). This slight shift in CDS sensitivity may be attributed to extended steric hindrance of ribosomes by the presence of additional factors, e.g., Hfq protein that associates with RybB and *ompN* mRNA in vivo (Sittka et al., 2008).

The five codon window proposed here may appear narrow, yet it can provide a large sequence space for translational control by sRNAs. First, sRNA-target duplexes are typically <15 bp (e.g., Argaman and Altuvia, 2000; Massé and Gottesman, 2002; Papenfort et al., 2008; Sharma et al., 2007; Udekwu et al., 2005; Vecerek et al., 2007), and core interactions down to six consecutive base pairs have been reported (Kawamoto et al., 2006). Second, the drive to maintain the amino acid sequence of a protein limits the mutation rate in the CDS; it will therefore also limit alterations to a sRNA target site in the CDS. Third, large-scale experiments using hundreds of expression constructs showed that efficient mRNA translation requires the first codons of mRNAs to be unstructured (Voges et al., 2004); this should favor sRNA-mediated control in precisely this domain, since these regulators often recognize single-stranded mRNA regions.

We believe that the RybB-*ompN* interaction is not an isolated case. In fact, the study of other RybB targets has predicted core interactions in the 5′ CDS, e.g., *ompW* (Johansen et al., 2006; and F.M., C.M.S., M.B., and J.V., unpublished data). *E. coli* OmrA sRNA also interacts mostly with the 5′ CDS of its *ompT* target mRNA; it is noteworthy that, similar to RybB, the 5′ residues of OmrA that pair with the *ompT* CDS are strongly conserved (Guillier and Gottesman, 2008). Interestingly, *Bacillus subtilis* SR1 RNA was found to inhibit 30S association of the *ahrC* target mRNA much further downstream in the CDS, i.e., starting from +80 (Heidrich et al., 2007). However, this case is not necessarily at loggerheads with our five codon window, for SR1 induces structural changes downstream of the *ahrC* start codon (Heidrich et al., 2007). Obviously, targeting the CDS would also provide a means for sRNAs to control the translation of mRNAs lacking SD sequences, i.e., the class of leaderless mRNAs (Moll et al., 2002).

Much remains to be learned about the mechanistic details of 30S interference in the CDS. For example, the toeprinting assays employed in this study scored for antisense inhibition of ternary complex formation. Whether RybB also interferes with the initial SD contact of 30S with the *ompN* mRNA, i.e., prior to stabilization by $tRNA^{fMet}$/AUG pairing, is as yet unknown. However, even if the formation of this binary complex were unabated, RybB might still prevent the *ompN* start codon from reaching the P site and thus affect the transition to the stable ternary complex. Recent cryo-electron microscopy snapshots of ribosomal complexes of *rpsO* mRNA, either unfolded or entrapped by S15 autorepressor protein, have revealed that S15 can stall the *rpsO* mRNA on the 30S subunit by precisely this mechanism, i.e., preventing the accomodation step of initiation (*rpsO* start codon from falling into the P site position) (Marzi et al., 2007).

Small RNAs may constitute only one class of antisense regulators that potentially operate in the five codon window. Aside from the translational attenuators in bacterial mRNAs (Babitzke, 2004), a staggering number of *cis*-encoded RNA thermosensor (Johansson et al., 2002; Morita et al., 1999; Narberhaus et al., 2006) and metabolite-binding riboswitches (Nudler and Mironov, 2004; Winkler and Breaker, 2005) have been identified. While the study of these elements has focused much on alternative secondary structures around the ribosome binding site, it seems conceivable that intramolecular pairing between the 5′UTR and 5′ CDS region could contribute to the repression mediated by these elements.

EXPERIMENTAL PROCEDURES

Oligonucleotides and Plasmids

DNA oligonucleotides used for cloning, PCR amplification of T7 templates, toeprinting assays, and antisense scanning are listed in Table S1. Plasmids used in this study are described in Table 1. Details of plasmid construction and expressed inserts are given in the Supplemental Data.

Bacterial Strains, Media, and Growth Conditions

Bacterial strains are listed in Table S2. The Δ*rybB* mutant of *E. coli* TOP10 (strain JVS-2398) was generated using the λ red protocol (Datsenko and Wanner, 2000), using primers JVO-2062/-2063 to amplify the kanamycin resistance cassette of plasmid pKD4. Successful *rybB* deletion was verified by colony PCR with oligos JVO-2064/-2065.

Growth in Luria-Bertani (LB) broth or on LB plates at 37°C was used throughout this study unless stated otherwise. SOC medium was used to recover transformants after heat shock or electroporation and prior to plating.

Table 1. Plasmids Used in This Study

Name	Expressed RNA	Comment	Origin/Marker	Reference
pXG10	*gfp* mRNA	GFP fusion vector, $P_{LtetO-1}$ promoter	pSC101*/Cm^R	Urban and Vogel, 2007
pZE12-luc	*luc* mRNA	general expression vector, P_{LlacO} promoter	ColE1/Amp^R	Lutz and Bujard, 1997
pJV300		sRNA control vector, expresses an ~50 nt nonsense transcript derived from *rrnB* terminator	ColE1/Amp^R	Sittka et al., 2007
pKP17-1	RybB	*Salmonella rybB* is under control of P_{BAD} promoter	pBR322/Amp^R	Papenfort et al., 2006
pFM7-5	*ompN::gfp*	$P_{LtetO-1}$-driven translational *ompN::gfp* fusion	pSC101*/Cm^R	this study
pFM33-1	$ompN_{M2}$*::gfp*	as above, but nucleotide G + 19 of *ompN* mutated to C	pSC101*/Cm^R	this study
pMB3	*ompN[B + 8]::gfp*	$P_{LtetO-1}$-driven translational *ompN[B+8]::gfp* fusion	pSC101*/Cm^R	this study
pMB4	*ompN[B + 11]::gfp*	$P_{LtetO-1}$-driven translational *ompN[B+11]::gfp* fusion	pSC101*/Cm^R	this study
pMB5	*ompN[B + 14]::gfp*	$P_{LtetO-1}$-driven translational *ompN[B+14]::gfp* fusion	pSC101*/Cm^R	this study
pMB1-1	*ompN[B + 17]::gfp*	$P_{LtetO-1}$-driven translational *ompN[B+17]::gfp* fusion	pSC101*/Cm^R	this study
pMB6	*ompN[B + 20]::gfp*	$P_{LtetO-1}$-driven translational *ompN[B + 20]::gfp* fusion	pSC101*/Cm^R	this study
pFM1-1	RybB	constitutive RybB RNA expression from P_{LlacO}	ColE1/Amp^R	this study
pFM17-2	RybB M2	constitutive RybB-M2 (C_2 to G change) RNA expression from P_{LlacO}	ColE1/Amp^R	this study
pFM46-1	R16TMA	constitutive expression (P_{LlacO}) of RybB residues 1–16 fused to residue +23 of *Salmonella micA* gene	ColE1/Amp^R	this study
pFM100-2	R16TOM	constitutive expression (P_{LlacO}) of RybB residues 1–16 fused to residue +24 of *Salmonella omrB*	ColE1/Amp^R	this study
pJV871	MicA	constitutive expression (P_{LlacO}) of *Salmonella micA* gene	ColE1/Amp^R	this study
pVP137	OmrB	constitutive expression (P_{LlacO}) of *Salmonella omrB* gene	ColE1/Amp^R	this study
pFS134	TOM	constitutive expression (P_{LlacO}) of truncated *Salmonella omrB* gene (starting at +16 position)	ColE1/Amp^R	this study
pFS135	TMA	constitutive expression (P_{LlacO}) of truncated *Salmonella omrB* gene (starting at +23 position)	ColE1/Amp^R	this study
pMB-2	B + 17TOM	constitutive expression (P_{LlacO}) of artificial TOM-based sRNA targeting the chimeric B + 17 mRNA near AUG (Figure S3)	ColE1/Amp^R	this study

Antibiotics (where appropriate) were applied at the following concentrations: 100 μg/ml ampicillin, 50 μg/ml kanamycin, and 20 μg/ml chloramphenicol.

Western Blot

Culture samples were taken according to 1 OD_{600}. Samples were spun 4 min at 16,100 × g at 4°C. The cell pellet was resuspended in 1× sample loading buffer (1 × SLB; Fermentas) to a final concentration of 0.01 OD/μl. Samples were heated 5 min at 95°C. Whole-cell fractions (0.1 OD) were separated via SDS PAGE. GFP and GroEL proteins were detected as described (Urban and Vogel, 2007).

T7 Transcription, Purification, 5′ End Labeling of RNA, and Footprinting

In vitro RNA synthesis using T7 RNA polymerase was done as described in Sittka et al. (2007) and 5′ end labeling of RNA as in Papenfort et al. (2006). The DNA template for *ompN* RNA in vitro transcription with T7 RNA polymerase was generated with the primers JVO-1244/-1245 on genomic DNA of *Salmonella* strain SL1344. It starts with a T7 promoter fused to the +1 transcriptional start site of *ompN* at position −75 relative to the *ompN* AUG start codon and ends with the 29th codon. The RybB DNA template was amplified using oligos JVO-1242/-1243. Sequences of the *ompN* and RybB RNAs are given in Table S3. DNA templates for *gltI* (−87 to +74) and *ompC* (−77 to +99) RNAs were amplified with primer pairs JVO-1039/-1040 and JVO-1246/-1247, respectively. The DNA templates used to generate the *ompN* RNA containing the shifted RybB-binding site and the *ompC* SD-N and *ompN* SD-C leaders were synthesized by two-step PCR. The first round of PCR amplified individual fragments of the 5′UTR and of the CDS of the respective DNA templates used for T7 transcription above. Substitution or addition of nucleotides was achieved by the amplification primers. The two generated PCR fragments were fused by a second round of PCR and facilitated by addition of short complementary sequences added by the primers in the first PCR step (DNA templates, a 1:1 ratio of the PCR products generated in the first step). The relevant primer pairs are summarized in Table S4. The sequences of all in vitro synthesized RNAs are listed in Table S3.

The detailed protocol for structure probing and footprinting was published in Sharma et al. (2007). Footprinting samples and sequencing ladders were denatured for 3 min at 95°C prior to separation on 6% (*ompN*) or 12% (RybB) polyacrylamide/7M urea sequencing gels in 1 × TBE. Gels were dried and analyzed using a PhosphoImager (FLA-3000 Series; Fuji) and AIDA software.

Toeprinting Analysis

Toeprinting assays were carried out as described previously (Hartz et al., 1988; Udekwu et al., 2005); our detailed protocol was published in Sharma et al. (2007). Details of the *ompN* (same as for structure probing), *ompC*, and *gltI* RNA are given above. The 5′ end-labeled primer for cDNA synthesis in the toeprinting reactions was complementary to the following mRNA positions: JVO-1245 to +70 to +90 of *ompN* mRNA, JVO-1247 to +82 to +99 of *ompC* mRNA, and JVO-1040 to +60 to +74 of *gltI* mRNA.

Sequencing ladders (*gltI*, *ompC*, and *ompN*) were generated with the CycleReader DNA Sequencing Kit (#K1711) of Fermentas according to the manufacturer's protocol using the same PCR-generated DNA template for RNA synthesis and the same 5′ end-labeled primer as for the toeprinting reactions (see below). cDNAs and sequence ladders were separated on a 6% polyacrylamide/7M urea gel. The gel was dried and analyzed using a PhosphorImager (FLA-3000 Series, Fuji) and AIDA software (Raytest, Germany).

Antisense oligos for interference with 30S binding were designed with a common melting temperature of approximately 48°C–53°C (see Table S1). 5R16 RNA (5′-GCCACUGCUUUUCUUU-3′) was chemically synthesized by

RiboTask ApS (Odense, Denmark). We determined in control experiments (mRNA and reverse transcriptase in toeprinting buffer; data not shown) that the addition of antisense DNA or RNA oligonucleotides per se did not affect reverse transcription of template RNAs (data not shown). Therefore, observed reductions of toeprinting signals in the antisense scanning experiments are considered specific in terms of antisense-mediated inhibition of 30S binding.

SUPPLEMENTAL DATA

The Supplemental Data include Supplemental Experimental Procedures, seven figures, four tables, and Supplemental References and can be found with this article online at http://www.molecule.org/supplemental/S1097-2765(08)00807-1.

ACKNOWLEDGMENTS

We thank F. Seifert for technical assistance, V. Pfeiffer for plasmid construction, and E.G.H. Wagner for insightful comments on the manuscript. This work was supported by an EMBO long-term fellowship to M.B. and by funds from the DFG Priority Program SPP1258 Sensory and Regulatory RNAs in Prokaryotes.

Received: July 3, 2008
Revised: September 22, 2008
Accepted: October 21, 2008
Published: December 24, 2008

REFERENCES

Argaman, L., and Altuvia, S. (2000). fhlA repression by OxyS RNA: kissing complex formation at two sites results in a stable antisense-target RNA complex. J. Mol. Biol. *300*, 1101–1112.

Babitzke, P. (2004). Regulation of transcription attenuation and translation initiation by allosteric control of an RNA-binding protein: the Bacillus subtilis TRAP protein. Curr. Opin. Microbiol. *7*, 132–139.

Beyer, D., Skripkin, E., Wadzack, J., and Nierhaus, K.H. (1994). How the ribosome moves along the mRNA during protein synthesis. J. Biol. Chem. *269*, 30713–30717.

Bossi, L., and Figueroa-Bossi, N. (2007). A small RNA downregulates LamB maltoporin in Salmonella. Mol. Microbiol. *65*, 799–810.

Calogero, R.A., Pon, C.L., Canonaco, M.A., and Gualerzi, C.O. (1988). Selection of the mRNA translation initiation region by Escherichia coli ribosomes. Proc. Natl. Acad. Sci. USA *85*, 6427–6431.

Chen, S., Zhang, A., Blyn, L.B., and Storz, G. (2004). MicC, a second small-RNA regulator of Omp protein expression in Escherichia coli. J. Bacteriol. *186*, 6689–6697.

Chiaruttini, C., Milet, M., and Springer, M. (1996). A long-range RNA-RNA interaction forms a pseudoknot required for translational control of the IF3-L35-L20 ribosomal protein operon in Escherichia coli. EMBO J. *15*, 4402–4413.

Darfeuille, F., Unoson, C., Vogel, J., and Wagner, E.G. (2007). An antisense RNA inhibits translation by competing with standby ribosomes. Mol. Cell *26*, 381–392.

Datsenko, K.A., and Wanner, B.L. (2000). One-step inactivation of chromosomal genes in Escherichia coli K-12 using PCR products. Proc. Natl. Acad. Sci. USA *97*, 6640–6645.

Dontsova, O., Kopylov, A., and Brimacombe, R. (1991). The location of mRNA in the ribosomal 30S initiation complex; site-directed cross-linking of mRNA analogues carrying several photo-reactive labels simultaneously on either side of the AUG start codon. EMBO J. *10*, 2613–2620.

Franch, T., Thisted, T., and Gerdes, K. (1999). Ribonuclease III processing of coaxially stacked RNA helices. J. Biol. Chem. *274*, 26572–26578.

Geissmann, T.A., and Touati, D. (2004). Hfq, a new chaperoning role: binding to messenger RNA determines access for small RNA regulator. EMBO J. *23*, 396–405.

Gualerzi, C.O., Brandi, L., Caserta, E., Garofalo, C., Lammi, M., La Teana, A., Petrelli, D., Spurio, R., Tomsic, J., and Pon, C.L. (2001). Initiation factors in the early events of mRNA translation in bacteria. Cold Spring Harb. Symp. Quant. Biol. *66*, 363–376.

Guillier, M., and Gottesman, S. (2006). Remodelling of the Escherichia coli outer membrane by two small regulatory RNAs. Mol. Microbiol. *59*, 231–247.

Guillier, M., and Gottesman, S. (2008). The 5′ end of two redundant sRNAs is involved in the regulation of multiple targets, including their own regulator. Nucleic Acids Res. *36*, 6781–6794.

Hartz, D., McPheeters, D.S., Traut, R., and Gold, L. (1988). Extension inhibition analysis of translation initiation complexes. Methods Enzymol. *164*, 419–425.

Heidrich, N., Moll, I., and Brantl, S. (2007). In vitro analysis of the interaction between the small RNA SR1 and its primary target ahrC mRNA. Nucleic Acids Res. *35*, 4331–4346.

Hui, A., and de Boer, H.A. (1987). Specialized ribosome system: preferential translation of a single mRNA species by a subpopulation of mutated ribosomes in Escherichia coli. Proc. Natl. Acad. Sci. USA *84*, 4762–4766.

Huntzinger, E., Boisset, S., Saveanu, C., Benito, Y., Geissmann, T., Namane, A., Lina, G., Etienne, J., Ehresmann, B., Ehresmann, C., et al. (2005). Staphylococcus aureus RNAIII and the endoribonuclease III coordinately regulate spa gene expression. EMBO J. *24*, 824–835.

Hüttenhofer, A., and Noller, H.F. (1994). Footprinting mRNA-ribosome complexes with chemical probes. EMBO J. *13*, 3892–3901.

Jacob, W.F., Santer, M., and Dahlberg, A.E. (1987). A single base change in the Shine-Dalgarno region of 16S rRNA of Escherichia coli affects translation of many proteins. Proc. Natl. Acad. Sci. USA *84*, 4757–4761.

Johansen, J., Rasmussen, A.A., Overgaard, M., and Valentin-Hansen, P. (2006). Conserved small non-coding RNAs that belong to the sigma(E) regulon: role in down-regulation of outer membrane proteins. J. Mol. Biol. *364*, 1–8.

Johansson, H.E., Belsham, G.J., Sproat, B.S., and Hentze, M.W. (1994). Target-specific arrest of mRNA translation by antisense 2′-O-alkyloligoribonucleotides. Nucleic Acids Res. *22*, 4591–4598.

Johansson, J., Mandin, P., Renzoni, A., Chiaruttini, C., Springer, M., and Cossart, P. (2002). An RNA thermosensor controls expression of virulence genes in Listeria monocytogenes. Cell *110*, 551–561.

Kaminishi, T., Wilson, D.N., Takemoto, C., Harms, J.M., Kawazoe, M., Schluenzen, F., Hanawa-Suetsugu, K., Shirouzu, M., Fucini, P., and Yokoyama, S. (2007). A snapshot of the 30S ribosomal subunit capturing mRNA via the Shine-Dalgarno interaction. Structure *15*, 289–297.

Kawamoto, H., Koide, Y., Morita, T., and Aiba, H. (2006). Base-pairing requirement for RNA silencing by a bacterial small RNA and acceleration of duplex formation by Hfq. Mol. Microbiol. *61*, 1013–1022.

Laursen, B.S., Sorensen, H.P., Mortensen, K.K., and Sperling-Petersen, H.U. (2005). Initiation of protein synthesis in bacteria. Microbiol. Mol. Biol. Rev. *69*, 101–123.

Lease, R.A., Smith, D., McDonough, K., and Belfort, M. (2004). The small noncoding DsrA RNA is an acid resistance regulator in Escherichia coli. J. Bacteriol. *186*, 6179–6185.

Lutz, R., and Bujard, H. (1997). Independent and tight regulation of transcriptional units in Escherichia coli via the LacR/O, the TetR/O and AraC/I1–I2 regulatory elements. Nucleic Acids Res. *25*, 1203–1210.

Majdalani, N., Vanderpool, C.K., and Gottesman, S. (2005). Bacterial small RNA regulators. Crit. Rev. Biochem. Mol. Biol. *40*, 93–113.

Malmgren, C., Engdahl, H.M., Romby, P., and Wagner, E.G. (1996). An antisense/target RNA duplex or a strong intramolecular RNA structure 5′ of a translation initiation signal blocks ribosome binding: the case of plasmid R1. RNA *2*, 1022–1032.

Marzi, S., Myasnikov, A.G., Serganov, A., Ehresmann, C., Romby, P., Yusupov, M., and Klaholz, B.P. (2007). Structured mRNAs regulate translation initiation by binding to the platform of the ribosome. Cell *130*, 1019–1031.

Massé, E., and Gottesman, S. (2002). A small RNA regulates the expression of genes involved in iron metabolism in Escherichia coli. Proc. Natl. Acad. Sci. USA *99*, 4620–4625.

Massé, E., Escorcia, F.E., and Gottesman, S. (2003). Coupled degradation of a small regulatory RNA and its mRNA targets in Escherichia coli. Genes Dev. *17*, 2374–2383.

Massé, E., Vanderpool, C.K., and Gottesman, S. (2005). Effect of RyhB small RNA on global iron use in Escherichia coli. J. Bacteriol. *187*, 6962–6971.

Mizuno, T., Chou, M.Y., and Inouye, M. (1984). A unique mechanism regulating gene expression: translational inhibition by a complementary RNA transcript (micRNA). Proc. Natl. Acad. Sci. USA *81*, 1966–1970.

Moll, I., Grill, S., Gualerzi, C.O., and Blasi, U. (2002). Leaderless mRNAs in bacteria: surprises in ribosomal recruitment and translational control. Mol. Microbiol. *43*, 239–246.

Møller, T., Franch, T., Udesen, C., Gerdes, K., and Valentin-Hansen, P. (2002). Spot 42 RNA mediates discoordinate expression of the E. coli galactose operon. Genes Dev. *16*, 1696–1706.

Morita, M.T., Tanaka, Y., Kodama, T.S., Kyogoku, Y., Yanagi, H., and Yura, T. (1999). Translational induction of heat shock transcription factor sigma32: evidence for a built-in RNA thermosensor. Genes Dev. *13*, 655–665.

Morita, T., Mochizuki, Y., and Aiba, H. (2006). Translational repression is sufficient for gene silencing by bacterial small noncoding RNAs in the absence of mRNA destruction. Proc. Natl. Acad. Sci. USA *103*, 4858–4863.

Murakawa, G.J., and Nierlich, D.P. (1989). Mapping the lacZ ribosome binding site by RNA footprinting. Biochemistry *28*, 8067–8072.

Narberhaus, F., Waldminghaus, T., and Chowdhury, S. (2006). RNA thermometers. FEMS Microbiol. Rev. *30*, 3–16.

Nudler, E., and Mironov, A.S. (2004). The riboswitch control of bacterial metabolism. Trends Biochem. Sci. *29*, 11–17.

Papenfort, K., Pfeiffer, V., Mika, F., Lucchini, S., Hinton, J.C., and Vogel, J. (2006). sigma(E)-dependent small RNAs of Salmonella respond to membrane stress by accelerating global omp mRNA decay. Mol. Microbiol. *62*, 1674–1688.

Papenfort, K., Pfeiffer, V., Lucchini, S., Sonawane, A., Hinton, J.C., and Vogel, J. (2008). Systematic deletion of Salmonella small RNA genes identifies CyaR, a conserved CRP-dependent riboregulator of OmpX synthesis. Mol. Microbiol. *68*, 890–906.

Platt, T., and Yanofsky, C. (1975). An intercistronic region and ribosome-binding site in bacterial messenger RNA. Proc. Natl. Acad. Sci. USA *72*, 2399–2403.

Rasmussen, A.A., Eriksen, M., Gilany, K., Udesen, C., Franch, T., Petersen, C., and Valentin-Hansen, P. (2005). Regulation of ompA mRNA stability: the role of a small regulatory RNA in growth phase-dependent control. Mol. Microbiol. *58*, 1421–1429.

Rehmsmeier, M., Steffen, P., Hochsmann, M., and Giegerich, R. (2004). Fast and effective prediction of microRNA/target duplexes. RNA *10*, 1507–1517.

Ringquist, S., MacDonald, M., Gibson, T., and Gold, L. (1993). Nature of the ribosomal mRNA track: analysis of ribosome-binding sites containing different sequences and secondary structures. Biochemistry *32*, 10254–10262.

Romby, P., Vandenesch, F., and Wagner, E.G. (2006). The role of RNAs in the regulation of virulence-gene expression. Curr. Opin. Microbiol. *9*, 229–236.

Schmidt, M., Zheng, P., and Delihas, N. (1995). Secondary structures of Escherichia coli antisense micF RNA, the 5′-end of the target ompF mRNA, and the RNA/RNA duplex. Biochemistry *34*, 3621–3631.

Sharma, C.M., Darfeuille, F., Plantinga, T.H., and Vogel, J. (2007). A small RNA regulates multiple ABC transporter mRNAs by targeting C/A-rich elements inside and upstream of ribosome-binding sites. Genes Dev. *21*, 2804–2817.

Shine, J., and Dalgarno, L. (1974). The 3′-terminal sequence of Escherichia coli 16S ribosomal RNA: complementarity to nonsense triplets and ribosome binding sites. Proc. Natl. Acad. Sci. USA *71*, 1342–1346.

Sittka, A., Pfeiffer, V., Tedin, K., and Vogel, J. (2007). The RNA chaperone Hfq is essential for the virulence of Salmonella typhimurium. Mol. Microbiol. *63*, 193–217.

Sittka, A., Lucchini, S., Papenfort, K., Sharma, C.M., Rolle, K., Binnewies, T.T., Hinton, J.C., and Vogel, J. (2008). Deep sequencing analysis of small noncoding RNA and mRNA targets of the global post-transcriptional regulator, Hfq. PLoS Genet. *4*, e1000163. 10.1371/journal.pgen.1000163.

Steitz, J.A. (1969). Polypeptide chain initiation: nucleotide sequences of the three ribosomal binding sites in bacteriophage R17 RNA. Nature *224*, 957–964.

Steitz, J.A., and Jakes, K. (1975). How ribosomes select initiator regions in mRNA: base pair formation between the 3′ terminus of 16S rRNA and the mRNA during initiation of protein synthesis in Escherichia coli. Proc. Natl. Acad. Sci. USA *72*, 4734–4738.

Storz, G., Opdyke, J.A., and Zhang, A. (2004). Controlling mRNA stability and translation with small, noncoding RNAs. Curr. Opin. Microbiol. *7*, 140–144.

Takyar, S., Hickerson, R.P., and Noller, H.F. (2005). mRNA helicase activity of the ribosome. Cell *120*, 49–58.

Thompson, K.M., Rhodius, V.A., and Gottesman, S. (2007). SigmaE regulates and is regulated by a small RNA in Escherichia coli. J. Bacteriol. *189*, 4243–4256.

Tjaden, B., Goodwin, S.S., Opdyke, J.A., Guillier, M., Fu, D.X., Gottesman, S., and Storz, G. (2006). Target prediction for small, noncoding RNAs in bacteria. Nucleic Acids Res. *34*, 2791–2802.

Udekwu, K.I., Darfeuille, F., Vogel, J., Reimegard, J., Holmqvist, E., and Wagner, E.G. (2005). Hfq-dependent regulation of OmpA synthesis is mediated by an antisense RNA. Genes Dev. *19*, 2355–2366.

Urban, J.H., and Vogel, J. (2007). Translational control and target recognition by Escherichia coli small RNAs in vivo. Nucleic Acids Res. *35*, 1018–1037.

Vecerek, B., Moll, I., and Blasi, U. (2007). Control of Fur synthesis by the non-coding RNA RyhB and iron-responsive decoding. EMBO J. *26*, 965–975.

Voges, D., Watzele, M., Nemetz, C., Wizemann, S., and Buchberger, B. (2004). Analyzing and enhancing mRNA translational efficiency in an Escherichia coli in vitro expression system. Biochem. Biophys. Res. Commun. *318*, 601–614.

Vytvytska, O., Moll, I., Kaberdin, V.R., von Gabain, A., and Bläsi, U. (2000). Hfq (HF1) stimulates ompA mRNA decay by interfering with ribosome binding. Genes Dev. *14*, 1109–1118.

Winkler, W.C., and Breaker, R.R. (2005). Regulation of bacterial gene expression by riboswitches. Annu. Rev. Microbiol. *59*, 487–517.

Yusupova, G.Z., Yusupov, M.M., Cate, J.H., and Noller, H.F. (2001). The path of messenger RNA through the ribosome. Cell *106*, 233–241.